ELSEVIER

Thermochimica Acta 304/305 (1997) 219–228

thermochimica acta

Influence of the thermal conductivity on the C_p-determination by dynamic methods

Benedikt Schenker*, Fritz Stäger

TCL, Eidgenössische Technische Hochschule, CH-8092 Zurich, Switzerland

Received 25 August 1996; accepted 29 January 1997

Abstract

Modulated DSC, Dynamic DSC and steady-state DSC are three frequently used methods to determine the heat capacity. This paper investigates how the C_p-values obtained by these methods are influenced by the different thermal conductivity of the material used for calibration and as sample. A simple mathematical model of the DSC-instrument is derived and the obtained C_p-values are compared for different operating conditions of the instrument and for different samples. Experiments with different samples are also performed and compared with the simulation results. The results clearly show that the temperature distribution in the sample puts a higher limit on the useful frequencies. Recommendations for operating conditions for accurate C_p measurements are given. © 1997 Elsevier Science B.V.

1. Introduction

Determination of C_p-values by Differential Scanning Calorimetry (DSC) is a well established method [1]. The classical method of C_p-determination employs three DSC runs with a linear temperature profile. With these three runs, one with an empty pan, one with a well-known reference substance and one with the sample to analyse, the heat capacity can easily be determined. However, this method has the following substantial drawbacks: It depends crucially on the long-time stability of the baseline of the instrument between the three runs and it does not allow to measure the C_p-value during quasi-isothermal conditions. In order to avoid these problems, and to achieve other advantages which are not mentioned here, different dynamic methods were developed. All these methods use different non-linear temperature profiles and sophisticated mathematical methods to compute the C_p-values. The Modulated DSC (MDSC) employs a sinusoidal temperature profile and a discrete-fourier-transformation-based evaluation [2], the Dynamic DSC (DDSC) uses a piece-wise linear temperature profile and also a fourier-transformation based evaluation [3], whereas the steady-state DSC (SSADSC) employs a piece-wise linear temperature profile and a pseudo-steady-state evaluation [4]. These three different methods are available as software and hardware options for different commercially available instruments, the MDSC together with instruments from Thermal Analytical Instruments, the DDSC from Perkin-Elmer and the SSADSC from Mettler-Toledo. This paper compares the three methods for dynamic C_p-determination by simulating the instrument and the sample quite rigorously. Although the simulated instrument is of the heat-flow type, all results also apply equally for power-compensating instruments.

*Corresponding author. Tel.: +4116323059; Fax: +41 16321222; E-mail: schenker@tech.chem.ethz.ch and staeger@tech.chem.-ethz.ch.

PII S0040-6031(97)00095-6

Although it is well known that a large sample with limited thermal conductivity shows a too low apparent heat capacity, and that it is proposed to use this fact for determination of the thermal conductivity [5] the influence of the thermal conductivity for small samples was not investigated systematically so far.

2. DSC simulation

2.1. Simulation principle

In order to keep the simulation simple and the numerical overhead small, the DSC is implemented as linear, time-constant dynamic system. This avoids the difficulties of a numerical integration of the system, and allows to employ a more accurate analytical solution of the system of differential equations. Like in [6] the furnace, the sample and the reference holder are modelled as simple RC elements, but here the temperature distribution in the sample is described with a partial differential equation.

2.2. Simulation details

The modulation of the reference temperature set point in the case of MDSC is a sine wave, while for DDSC and SSADSC it is a saw-tooth function. These two functions are generated with the following differential equations:

$$\frac{dx_1}{dt} = x_2(t) \tag{1}$$

$$\frac{dx_2}{dt} = -\omega^2 x_1(t) \tag{2}$$

$$\frac{dx_3}{dt} = x_2(t) + u(t) \tag{3}$$

Depending on the choice of u and $x(0)$ the differential Eq. (1), Eq. (2) and Eq. (3) either generate a sine wave or a saw-tooth function. The sine wave is yield for $u=0$, $x_1(0)=0$, $x_2(0)=\omega$, and $x_3(0)=0$, with $\omega=2\pi/t_p$, and the saw-tooth for $x_1(0)=x_2(0)=0$ and $x_3(0)=1$ with $u=-4/t_p$ for the first half of the period, and $u=4/t_p$ for the second. t_p is the period duration. This generator for the reference temperature set-point T_P, using x_3 as T_P, has the advantage that both signals can be yielded with the same system, and that this system can be exactly represented in the discrete-time domain with a zero order hold on u, as long as the period duration t_p is an even multiple of the sampling time Δt.

The temperature control system, consisting of the furnace and the reference is simulated using the following differential equation:

$$\frac{dx_4}{dt} = \frac{dT_R}{dt} = \tau_R(T_F - T_R) \tag{4}$$

were τ_R is the time constant of the reference temperature. The reference temperature T_R is controlled by a P-controller:

$$T_F = T_P + P(T_P - T_R) \tag{5}$$

were P is the proportional gain of the controller, T_P the reference temperature setpoint and T_F the furnace temperature. With Eq. (4) and Eq. (5), the reference temperature is given by:

$$\frac{dx_4}{dt} = \frac{dT_R}{dt} = \tau_{R((P+1)}T_{P-(P+1)}T_R) \tag{6}$$

$$= \tau_R((P+1)x_3 - (P+1)x_4) \tag{7}$$

The temperature distribution in the sample is governed by thermal conduction, which is described by the following partial differential equation:

$$\frac{\partial^2 T}{\partial z^2} = \frac{\rho C_p}{\lambda} \cdot \frac{\partial T}{\partial t} \tag{8}$$

were ρ is the density, λ is the thermal conductivity and C_p the specific heat capacity of the sample.

Further assuming that the sample is heated only from the bottom and no heat is exchanged at the sides and at the top of the sample and discretizing Eq. (8) in the spatial dimension, the following ordinary differential equation describes a finite element of the sample:

$$\frac{dx_6}{dt} = \frac{dT_n}{dt} = \frac{A\lambda}{C_{p_n}\Delta z} \cdot \left(T_{(n-1)} - 2T_n - T_{(n+1)}\right) \tag{9}$$

Combining Eq. (5) and Eq. (9) yields the sample temperatures for the different finite elements and the value of the sample temperature measurement:

$$\frac{dx_5}{dt} = \frac{dT_S}{dt} = \tau_S((P+1)T_P - PT_R - T_S) + \left(\frac{2\lambda A}{\Delta z \cdot mC_{pS}}\right) \cdot T_{f1} \tag{10}$$

$$= \tau_S((P+1)x_3 - Px_4 - x_5)\left(\frac{2\lambda A}{\Delta z \cdot mC_{pS}}\right) \cdot x_6 \quad (11)$$

where τ_S is the time constant and mC_{pS} the mass times the heat capacity of the sample holder, A is the area and λ the thermal conductivity of the sample, and Δz is the thickness of the first finite element which has a temperature of T_{f1}. The temperatures of the inner finite elements are given by Eq. (9).

The above system can be written down in a matrix notation as:

$$\frac{dx}{dt} = Ax(t) + bu(t) \quad (12)$$

with

$$A = \begin{bmatrix} 0 & 1 & 0 & 0 & 0 & 0 & 0 & 0 & \dots \\ -\omega^2 & 0 & 0 & 0 & 0 & 0 & 0 & 0 & \dots \\ 0 & 1 & 0 & 0 & 0 & 0 & 0 & 0 & \dots \\ 0 & 0 & (P+1)\tau_R & -(P+1)\tau_R & 0 & 0 & 0 & 0 & \dots \\ 0 & 0 & (P+1)\tau_S & -P\tau_S & -\tau_S & -2\xi & 2\xi & 0 & \dots \\ 0 & 0 & 0 & 0 & 2\xi & -3\xi & \xi & 0 & \dots \\ 0 & 0 & 0 & 0 & 0 & \xi & -2\xi & \xi & \dots \\ \vdots & \vdots & \vdots & \vdots & \vdots & \vdots & \vdots & \vdots & \end{bmatrix}$$

$$\xi = \left(\frac{2\lambda A}{\Delta z \cdot mC_{p,n}}\right)$$

$$b = [0, 0, 1, 0, \dots, 0]^T$$

$$x = [x_1, x_2, T_P, T_R, T_S, T_{f1}, T_{f2}, \dots, T_{fN}]^T$$

This time-contiguous description can be transformed to a time-discrete linear system with a zero order hold assumption on the input u. Since the system is set up such that this zero-order hold does not introduce errors, it can be efficiently evaluated with very high accuracy.

Fig. 1 shows a schematic view of the simulated instrument and how it is represented by RC components. By simulating the sample as a large number of thin slices the ordinary differential equation approximates the partial equation more and more. The presented results were obtained using 10 finite elements. Using a larger number did not significantly change the results.

3. C_p-evaluation

The three compared methods use different excitations signals and employ different evaluation algorithms to determine the C_p-values. MDSC uses a sinusoidal temperature profile and employs a fourier transformation:

$$\mathscr{A} = \int_0^T (T_S - T_R) \cdot \sin(\omega \cdot t)dt + i \cdot \int_0^T (T_S - T_R) \cdot \cos(\omega \cdot t)dt$$

where i is $\sqrt{-1}$ and $\omega = 2 \cdot \pi / t_p$. The C_p of the sample is then calculated as:

$$C_p(MDSC) = \frac{|\mathscr{A}_{sample}|}{m_{sample}} \cdot \frac{mC_{p_{calibration}}}{|\mathscr{A}_{calibration}|}$$

where $|\mathscr{A}_{sample}|$ denotes the amplitude of the run with the sample, m_{sample} the mass of the sample, $|\mathscr{A}_{calibration}|$ the amplitude of the run with a calibration substance and $mC_{p_{calibration}}$ the mass times the heat capacity of the calibration substance.

DDSC uses a saw-tooth function as temperature profile and a discrete fourier transformation for evaluation. In contrast to the MDSC the C_p-evaluation for this method does not compare the amplitudes, but the

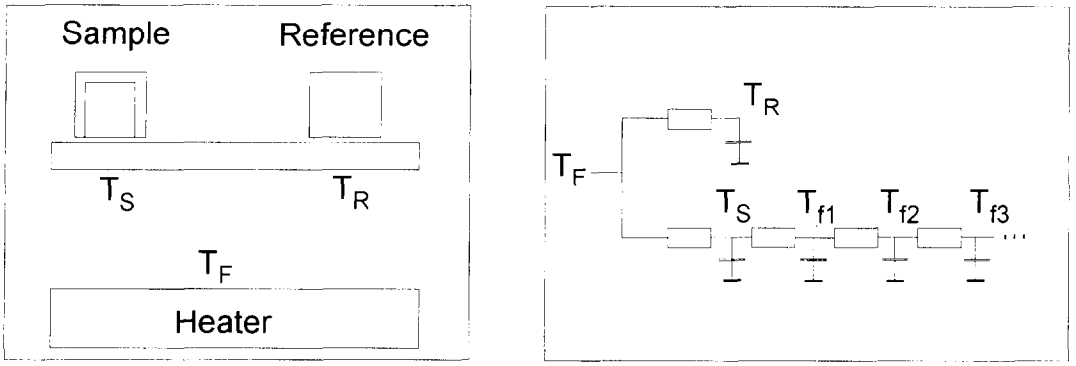

Fig. 1. Scheme of the simulated instrument and how it is represented by RC components.

only real parts of the (generally) complex amplitude.

$$C_p(DDSC) = \frac{Re(\mathscr{A}_{\text{sample}})}{m_{\text{sample}}} \cdot \frac{mC_{\text{p}}\text{calibration}}{Re(\mathscr{A}_{\text{calibration}})}$$

The calibration run also gives the phase lag of the instrument, which is taken into account by rotating the amplitude vectors such that the complex part of the $\mathscr{A}_{\text{calibration}}$ vanishes.

SSADSC also uses a saw-tooth function as temperature profile and evaluates the C_p simply by comparing the different temperature excursions:

$$C_{\text{p}}(SSADSC) = \frac{(\max(T_S - T_R) - \min(T_S - T_R))}{m_{\text{sample}}}\Big|_{\text{sample}} \cdot \frac{mC_{\text{p}_{\text{calibration}}}}{(\max(T_S - T_R) - \min(T_S - T_R))}\Big|_{\text{calibration}} \tag{16}$$

4. Simulation Results

The different C_p-determination methods are compared for different sample substances, aluminium, sapphire and polystyrene with disk diameters of 4 mm, and with polystyrene disks with 3 mm diameter. Table 1 summarises the physical properties of the sample substances, and Table 2 the parameters employed for the instrument simulation. For all the three methods compared a run with a 5 mg aluminium disk with 4 mm diameter as sample was used to calibrate the method. Based on these calibration factors the runs with the other samples were evaluated. Since the simulation assumes a perfect balanced instrument, no blank line had to be subtracted. Tables 3–6 and Fig. 2 summarise the results for the C_p-evaluations. For the very well heat-conducting sample of aluminium and the well heat-conducting sample of sapphire only relatively small errors are encountered, but for the polystyrene disk large errors can be observed, especially for short period durations and relatively large samples. For the parameters recommended by TAI for C_p-determination by MDSC [7], which recommends 10 to 20 mg of sample and oscillation periods between 60 and 100 s, errors up to 25% or the 4 mm disk and well over 50% for the 3 mm

Table 1
Physical properties of the samples investigated

Substance	Density [kg/m^3]	Thermal capacity [J/(kg·K)]	Thermal conductivity [W/(K·m)]
Aluminium	2700	896	239
Sapphire	3970	1000	34.7
Polystyrene	1000	1132	0.1506

Table 2
Parameters employed for the instrument simulation

Parameter	Unit	Value
τ_R	s^{-1}	0.084
τ_S	s^{-1}	0.084
P		20
mC_pS	$J \cdot K^{-1}$	0.24
N		10

Table 3
Relative errors of the C_p-evaluations in % for the different methods. Sample: Aluminium disks with 4 mm diameter

t_p	5 mg sample			10 mg sample			20 mg sample		
[s]	MDSC	DDSC	SSADSC	MDSC	DDSC	SSADSC	MDSC	DDSC	SSADSC
10	0.00	0.00	0.00	−1.79	−1.79	−1.85	−5.18	−5.19	−5.37
20	0.00	0.00	0.00	−1.70	−1.70	−1.70	4.94	−4.95	−4.93
40	0.00	0.00	0.00	−1.43	−1.43	−1.25	−4.19	−4.21	−3.69
60	0.00	0.00	0.00	−1.13	−1.14	−0.80	−3.34	−3.38	−2.41
80	0.00	0.00	0.00	−0.88	−0.88	−0.47	−2.60	−2.64	−1.44
100	0.00	0.00	0.00	−0.68	−0.68	−0.26	−2.03	−2.06	−0.81
120	0.00	0.00	0.00	−0.53	−0.53	−0.14	−1.60	−1.63	−0.43
160	0.00	0.00	0.00	−0.34	−0.35	−0.04	−1.04	−1.06	−0.12
320	0.00	0.00	0.00	−0.10	−0.10	0.00	−0.30	−0.31	0.00

Table 4
Relative errors of the C_p-evaluations in % for the different methods. Sample: Sapphire disks with 4 mm diameter

t_p	5 mg sample			10 mg sample			20 mg sample		
[s]	MDSC	DDSC	SSADSC	MDSC	DDSC	SSADSC	MDSC	DDSC	SSADSC
10	−0.21	−0.21	−0.23	−2.19	−2.20	−2.32	−5.93	−5.97	−6.33
20	−0.20	−0.20	−0.20	−2.09	−2.09	−2.10	−5.67	−5.69	−5.72
40	−0.17	−0.17	−0.15	−1.76	−1.76	−1.54	−4.81	−4.85	−4.26
60	−0.13	−0.13	−0.09	−1.39	1.40	0.99	−3.85	−3.89	−2.79
80	−0.10	−0.10	−0.05	−1.08	−1.08	−0.58	−3.00	−3.05	−1.67
100	−0.08	−0.08	−0.03	−0.83	−0.84	−0.32	−2.34	−2.39	−0.94
120	−0.06	−0.06	−0.02	−0.65	−0.66	−0.17	−1.85	−1.89	−0.51
160	−0.04	−0.04	0.00	−0.42	−0.43	−0.04	−1.20	−1.23	−0.14
320	−0.01	−0.01	0.00	−0.12	−0.12	0.00	−0.35	−0.36	0.00

Table 5
Relative errors of the C_p-evaluation in % for the different methods. Sample : Polystyrene disks with 4 mm diameter

t_p	5 mg sample			10 mg sample			20 mg sample		
[s]	MDSC	DDSC	SSADSC	MDSC	DDSC	SSADSC	MDSC	DDSC	SSADSC
10	−4.45	−7.46	−5.82	−34.54	−48.50	−37.14	−71.24	−79.98	−73.33
20	−1.55	−2.37	−5.53	−15.48	−23.20	−19.47	−57.31	−69.89	−61.03
40	−0.70	−0.92	−2.09	−6.33	−9.11	−9.00	−36.50	−49.85	−38.82
60	−0.46	−0.57	−0.90	−3.82	−5.26	−4.48	−24.43	−35.18	−22.38
80	−0.33	−0.39	−0.42	−2.62	−3.51	−2.16	−17.26	−25.53	−12.73
100	−0.25	−0.29	−0.20	−1.91	−2.52	−1.06	−12.72	−19.11	−6.80
120	−0.19	−0.22	−0.09	−1.45	−1.89	−0.52	−9.69	−14.70	−3.56
160	−0.12	−0.14	0.02	−0.90	−1.16	−0.12	−6.07	−9.32	−0.94
320	−0.03	−0.04	0.00	−0.25	−0.32	0.00	−1.72	−2.68	0.00

disk can be yielded. Fig. 3 shows the temperature distribution in the sample and Fig. 4 the difference temperature signal for the 20 mg, 3 mm polystyrene sample. The significant lag of the temperature in the sample can clearly be seen, but due to the linearity of the system and the used excitation of a pure sine wave the measured signal is not perceptibly inaccurate, as the temperature difference signal shows.

Fig. 5 shows the maximal allowable thickness for a different values of the thermal diffusivity $\alpha=\lambda/(\rho\cdot C_p)$

Table 6
Relative errors of the C_p-evaluation in % for the different methods. Sample : Polystyrene disks with 3 mm diameter

t_p	5 mg sample			10 mg sample			20 mg sample		
[s]	MDSC	DDSC	SSADSC	MDSC	DDSC	SSADSC	MDSC	DDSC	SSADSC
10	−25.90	−38.72	−27.77	−66.96	−77.32	−69.59	−83.66	−88.92	−84.99
20	−9.57	−15.34	−13.25	−49.71	−63.88	−54.09	−77.12	−83.98	−79.01
40	−3.08	−4.87	−6.18	−27.27	−39.57	−29.56	−67.54	−77.49	−68.62
60	−1.60	−2.45	−2.59	−16.45	−24.99	−15.09	−58.81	−71.37	−57.12
80	−1.00	−1.50	−1.13	−10.86	−16.80	−7.68	−50.75	−64.87	−45.19
100	−0.69	−1.02	−0.51	−7.64	−11.94	−3.68	−43.59	−58.26	−34.32
120	−0.51	−0.73	−0.23	−5.64	−8.86	−1.76	−37.40	−51.90	−25.34
160	−0.30	−0.43	0.05	−3.41	−5.37	−0.40	−27.72	−40.69	−13.01
320	−0.08	−0.12	0.00	−0.92	−1.46	0.00	−10.20	−16.47	0.65

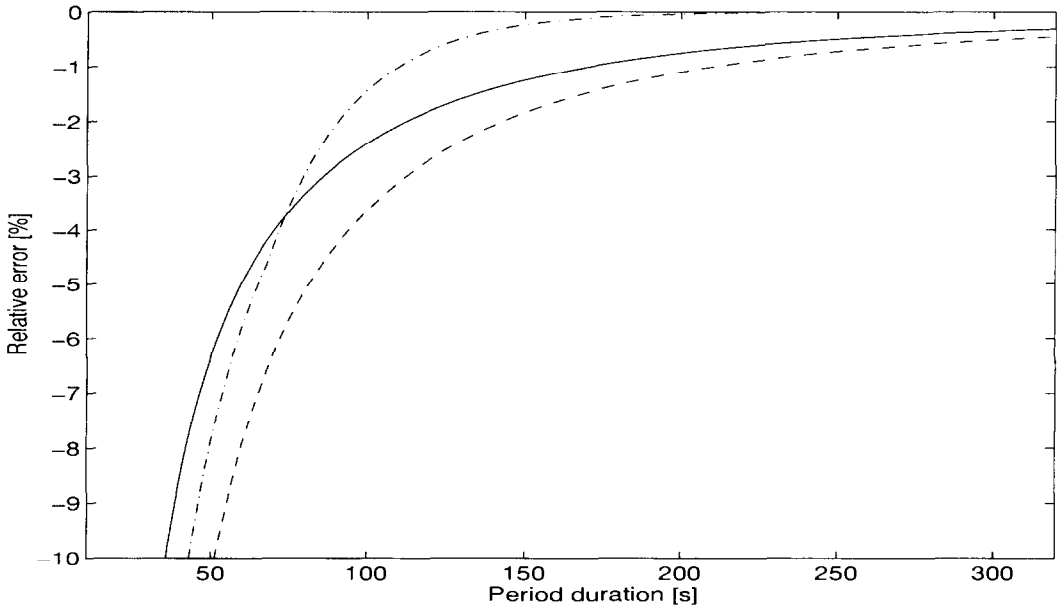

Fig. 2. Comparison of the different methods for a 4 mm polystyrene disk of 10 mg (——, MDSC; - - - -, DDSC; –.–.–, SSADSC).

that give errors smaller than 2% for the sinusoidal excitation. Again the importance of small samples is clearly visible.

5. Experimental investigations

The heat capacity of polystyrene and sapphire is measured for different period lengths using a sinusoidal temperature excitation with a Mettler DSC821e instrument. The polystyrene sample was cut from a plate and had a thickness of 1.34 mm and a footprint of 3×3.5 mm, with a mass of 12.755 mg. The sapphire sample was a circular disc with a thickness of 0.3 mm and a diameter of 4.5 mm, with a mass of 27.245 mg. The measurements are made quasi-isothermally at a temperature of 75°C. For each period length four DSC runs with the same crucibles are made:

- An empty run, without crucibles on either the sample nor the reference position.
- A blank run, with a crucible with a lid on the sample position and a crucible without a lid on the reference position.

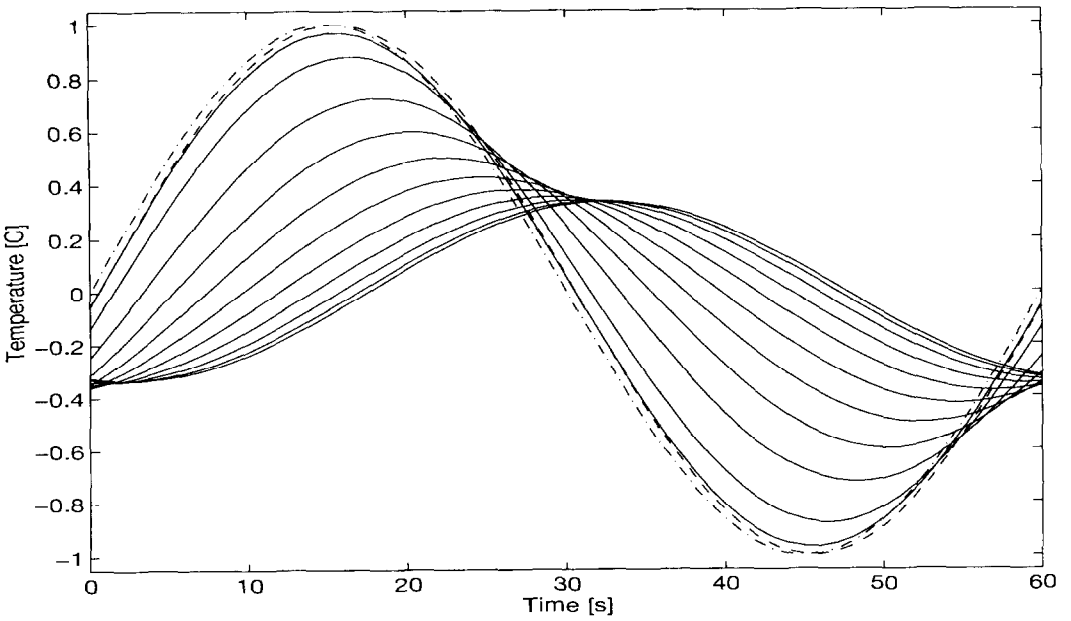

Fig. 3. Temperature distribution in a sample of 20 mg of polystyrene, 60 s period duration (——, temperatures of the different finite elements; - - - -, T_R; –.–.–, T_P).

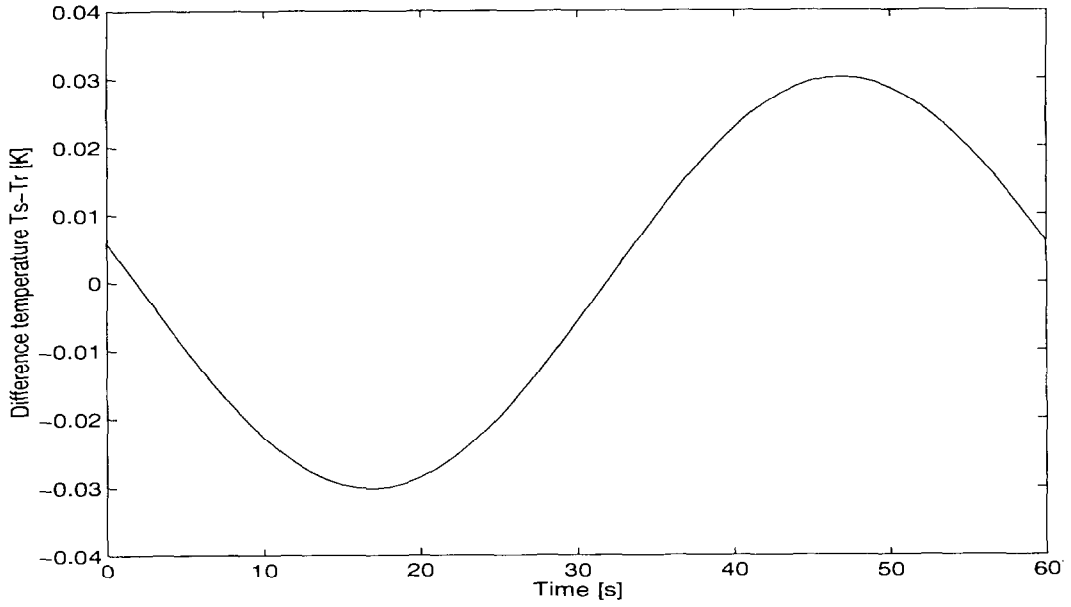

Fig. 4. Temperature difference signal T_S–T_R from the sample of Fig. 3.

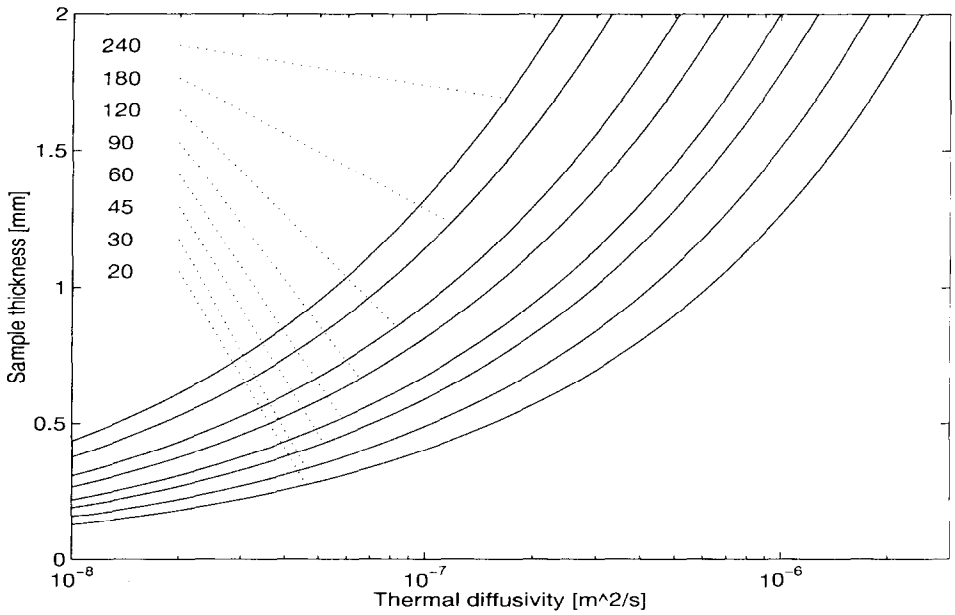

Fig. 5. Maximal thickness of the sample for errors less than 2% for different values of the thermal diffusivity $\alpha = \lambda/(\rho \cdot c_p)$ and different period durations in seconds for the sinusoidal excitation.

- Two measurements runs with the sapphire, respectively with the polystyrene, samples.

Based on these measurements the heat capacities are computed, using two different algorithms:

- C_p**(corr)** – The empty run and the blank run are employed for calibration of the DSC-cell and for compensation of the cell asymmetry.
- C_p**(conv)** – Only the cell asymmetry is compensated.

The calculations are done with the software of the DSC821e.

Table 7 and Fig. 6 show the results of single measurements for different period lengths. It can be clearly seen that the relatively thick 1.3 mm polystyrene sample, even with relatively long period durations, shows a C_p value that is significantly too low. The agreement between the simulation and the measurements is satisfactory. The differences can be explained by the fact that the simulation is based on the assump-

Table 7
Results of the measurements

Period duration [s]	Measurements polystrene C_p (corr) [J/(gK)]	Deviation from literature value [%]	Measurement sapphire C_p (corr) [J/(gK)]	Deviation from literature value [%]
20	0.75	−48.9	0.69	−20.2
30	1.00	−31.4	0.78	−10.4
45	1.17	−19.7	0.85	−1.6
60	1.31	−10.0	0.88	1.3
90	1.37	−6.2	0.89	2.5
120	1.38	−5.5	0.88	1.2
180	1.42	−2.3	0.89	2.2
240	1.43	−1.6	0.86	−0.9

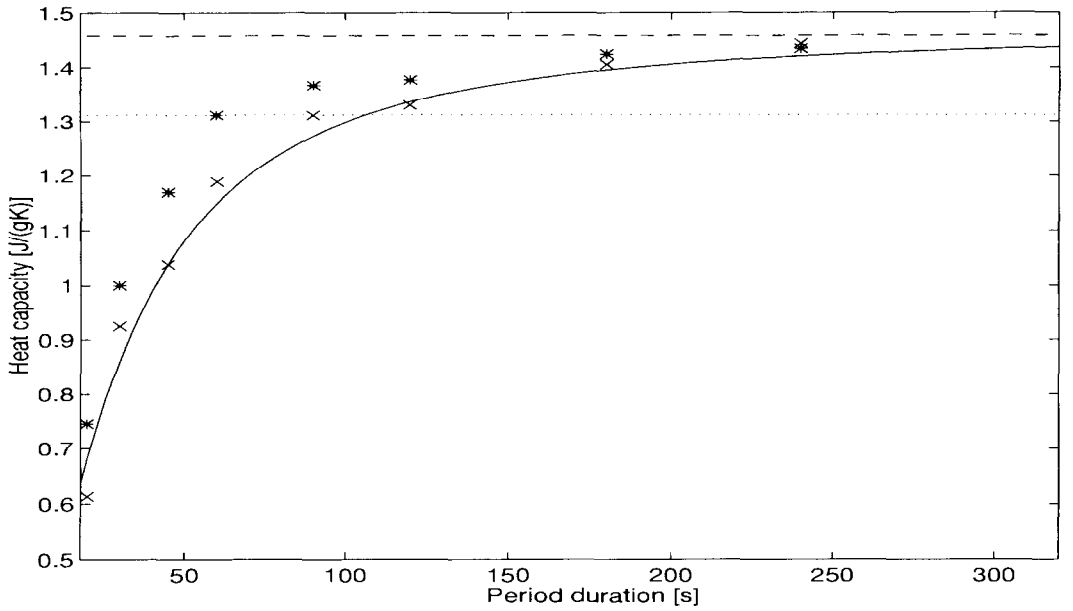

Fig. 6. Results of the measurements and the simulation for polystyrene at 75°C (- - - -, literature value polystyrene; . . . . ., literature value polystyrene −10%; ——, simulated values; *, c_p(corr); ×, c_p(conv)).

tion that the heat is transferred only via the base area of the sample and not by the other surfaces. As in the actual measurement the heat is also transferred by the other surfaces, however, this leads to a lower influence of the thermal conductivity. The results for sapphire in Table 7 show that the DSC furnace can readily propagate the modulation down to a period duration of 30 s.

Fig. 6 also clearly shows the effect of the correction by the empty and the blank run when C_p(corr) is compared with C_p(conv). An additional sapphire run is not needed.

6. Conclusions

Accurate determination of the C_p-values in polymers or other poor heat conductors requires relatively long period durations in the order of 3 to 6 min, even if small samples with a large surface and a good thermal contact are used, because for shorter period durations the temperature distribution in the sample is too heterogeneous. Note that these period durations are required due to the thermal conductivity in the sample, and not by the dynamics of the employed instrument. Even with an instrument able to use much shorter period durations the sample precludes the application of these shorter durations. Furthermore it is important to realise that measures which improve the thermal contact between the sample and the instrument, like using Helium as purge gas, do not help to get a more uniform temperature distribution within the sample. On the other hand, using crimped pans would allow to use slightly larger samples, or slightly shorter period durations, due to the added heat flow through the crimped lid.

For the same accuracy MDSC and DDSC require generally longer period durations. The possibly poor accuracy of the MDSC measurements cannot be seen on the measured curves and has to be detected by repeated measurements with other period durations. The DDSC method does not fundamentally improve the accuracy but the saw-tooth excitation has a smaller amplitude of the basic frequency used afterwards in the evaluation, for the same temperature scan. The saw-tooth excitation employed in the DDSC and the SSADSC method allow for an easy optical judgement to decide if the period duration is long enough to reach a pseudo-steady state.

From the, somewhat idealised, simulation it can be derived that the SSADSC method yields the most accurate results. In real measurements many other

factors like noise, non-linearity, disturbances of the controllers and so forth also influence the results. However, it is to be expected that most of these factors do not either favour any of the methods or affect the SSADSC method only to a lesser degree.

References

[1] B. Wunderlich, Thermal Analysis, Academic Press, New York (1990).

[2] M. Reading, D. Elliot and V. Hill, 21st NATAS (1992) pp. 145–150.

[3] J.E.K. Schawe, Thermochimica Acta, 260 (1995) 1–16.

[4] K.Krewson, B. Schenker and J. de Buhr, 11th ICTAC, (1996) p. 230.

[5] S.M. Marcus and R.L. Blaine, 22nd NATAS, (1993) pp. 102-108 .

[6] U. Ulbrich and H. Cammenga, Thermochimica Acta, 229 (1993) 53–67.

[7] Thermal Analytical Instruments, Thermal Applications Note, Heat Capacity by Modulated DSC..